29 October 1999

ELSEVIER

Chemical Physics Letters 312 (1999) 511–521

CHEMICAL PHYSICS LETTERS

www.elsevier.nl/locate/cplett

Decomposition of exchange-correlation energies

Andrew T.B. Gilbert *, Peter M.W. Gill

Department of Chemistry, University of Cambridge, Cambridge CB2 1EW, UK

Received 13 May 1999; in final form 22 July 1999

Abstract

We discuss a function $Q(x)$ that decomposes a locally defined exchange-correlation energy of a system into contributions from each value of the reduced density gradient x. We outline a method for constructing these functions for molecular systems and give examples of these for the Dirac exchange energy of some simple molecules. Graphs of the $Q(x)$ functions show which values of the reduced gradient are the most important energetically. We use the curves to construct an ab initio gradient-corrected exchange functional which yields the exact energy for a new model reference density. The performance of this functional when applied to chemical systems is examined.

1. Introduction

There can be little doubt that density functional theory (DFT) is now the most popular approach to computational quantum chemistry. Its relatively modest computational cost and the high accuracy often achieved by modern exchange-correlation (XC) functionals provide an attractive combination which, in recent years, has largely replaced the more traditional Hartree–Fock (HF)-based methods. This shift in allegiance has both fostered, and been fostered by, the inclusion of DFT capabilities in modern quantum-chemistry computer programs.

Understanding, however, has proved to be more elusive than popularity; to the majority of its adherents and advocates, DFT is still a black box that works. This pragmatic mindset is not entirely a bad thing for it has propelled the successful application of DFT to an enormous range of problems, but we should not lose sight of the fundamental questions that remain only partially answered and the pursuit of deeper understanding should never be abandoned.

Recently, the desire for greater accuracy has led to an increase in the level of parameterisation in density functionals. Nearly all those in common use today, and certainly those professing the greatest accuracy, incorporate a number of parameters that have been chosen to minimise the error associated with some benchmark data set [1–3]. This approach is augmented by an arsenal of scaling relationships and asymptotic conditions which are used to determine the form of the functional [4,5], but the sea of parameters can cloud the real reasons for their success.

* Corresponding author.Fax: +44-115-9513562; e-mail: atg@theor.ch.cam.ac.uk

0009-2614/99/$ - see front matter
PII: S0009-2614(99)00836-2

Ab initio functionals avoid this empiricism, and their successes or failures can be directly traced either to the quality of the reference system upon which they are based or to assumptions made in their derivation. Although the performance of ab initio functionals [6–9] is inferior to that of their parameterised counterparts for molecules, the work of Dirac and others on the uniform electron gas (UEG) remains the foundation stone upon which many other functionals are built, and the continued use of these results testifies to the enduring worthiness of such exact treatments.

In this Letter, we explore a new approach to the construction of an ab initio density functional for exchange. It relies on an energy decomposition that was first introduced by Zupan et al. [10,11] and which we briefly review in Section 2. This decomposition may be applied to any energy that is defined locally, but we restrict our treatment to DFT exchange energies. We present examples of this decomposition for hydrogenic densities and small molecules in Sections 3 and 4, and use it in Section 5 to derive a new functional. Sections 6 and 7 contain comparisons of the performance this new functional with other published ab initio functionals and the conclusions of this work.

2. General theory

Many of the popular exchange functionals can be written in the form

$$E_X = \int \rho(\boldsymbol{r})^{4/3} g(x(\boldsymbol{r}))\, \mathrm{d}\boldsymbol{r} \tag{1}$$

where the integral is over all space and ρ is an electron spin density of the system. The dimensionless quantity x is defined by

$$x(\boldsymbol{r}) = \frac{|\nabla\rho(\boldsymbol{r})|}{\rho(\boldsymbol{r})^{4/3}} \tag{2}$$

and is often called the reduced gradient. It is a measure of the local deviation from uniformity of the density. The well-known Dirac and Becke functionals [6,4],

$$g_{\mathrm{D30}}(x) = -\frac{3}{2}\left(\frac{3}{4\pi}\right)^{1/3} \tag{3}$$

$$g_{\mathrm{B88}}(x) = -\frac{3}{2}\left(\frac{3}{4\pi}\right)^{1/3} - \frac{b x^2}{1 + 6\, b x \sinh^{-1}(x)} \tag{4}$$

($b = 0.0042$) are typical examples.

If we define the set Ω_χ by

$$\Omega_\chi = \{\boldsymbol{r} | x(\boldsymbol{r}) = \chi\} \tag{5}$$

then the three-dimensional integral over space in (1) may be transformed to a one-dimensional integral over χ

$$E_X = \int_0^\infty q(\chi)\, \mathrm{d}\chi \tag{6}$$

$$Q(\chi) = \int_{\Omega_\chi} \rho^{4/3}(\boldsymbol{r})\, g(x)\, \mathrm{d}\boldsymbol{r} \tag{7}$$

$Q(\chi)\,\mathrm{d}\chi$ therefore represents the contribution to E_X from all points in the molecule with reduced gradient between χ and $\chi + \mathrm{d}\chi$. One can interpret the function $Q(\chi)$, which we term a Q-curve, as a gradient

decomposition, or gradient spectrum, of the exchange energy of a given density. It shows explicitly which values of the reduced gradient are contributing to the energy.

If we consider single-electron systems, a similar function may be constructed for the Hartree–Fock (HF) exchange functional. In such systems, the exchange energy (which exactly cancels the spurious coulomb self-interaction) is given by

$$E_{\mathrm{K}} = \frac{1}{2}\int \rho(\boldsymbol{r}) V_{\mathrm{K}}(\boldsymbol{r})\ \mathrm{d}\boldsymbol{r} \tag{8}$$

where V_{K} is the exchange potential which, in single-electron systems takes the simple form

$$V_{\mathrm{K}}(\boldsymbol{r}) = -\int \frac{\rho(\boldsymbol{r}')}{|\boldsymbol{r}-\boldsymbol{r}'|}\ \mathrm{d}\boldsymbol{r}' \tag{9}$$

The resulting Q-curve is therefore

$$Q_{\mathrm{HF}}(\chi) = \frac{1}{2}\int_{\Omega_\chi} \rho(\boldsymbol{r}) V_{\mathrm{K}}(\boldsymbol{r})\ \mathrm{d}\boldsymbol{r} \tag{10}$$

For these systems, Eqs. (7) and (10) allow a direct comparison between HF theory and density functionals of the form (1), showing from where the energy is being contributed in each case.

3. Hydrogen-like ions

It is often illuminating to solve a transparently simple model system exactly. The density and reduced gradient of a hydrogen-like ion (H, $\mathrm{He}^{+}, \ldots$) with nuclear charge Z are

$$\rho = \frac{Z^3}{\pi}\exp(-2Zr) \tag{11}$$

$$x = 2\sqrt[3]{\pi}\exp(+2Zr/3) \tag{12}$$

and it can be shown that the resulting Q-curve for the exchange energy given by (1) is

$$\frac{Q_g(x)}{Z} = \begin{cases} 0 & 0 \leqslant x < 2\sqrt[3]{\pi} \\ g(x)\,\dfrac{24\,\pi}{x^5}\log^2\left(\dfrac{x^3}{8\,\pi}\right) & 2\sqrt[3]{\pi} \leqslant x \end{cases} \tag{13}$$

The corresponding HF Q-curve is

$$\frac{Q_{\mathrm{HF}}(x)}{Z} = \begin{cases} 0 & 0 \leqslant x < 2\sqrt[3]{\pi} \\ \dfrac{12\pi}{x^7}\log\left(\dfrac{x^3}{8\pi}\right)\left(x^3 - 8\pi - 4\pi\log\left(\dfrac{x^3}{8\pi}\right)\right) & 2\sqrt[3]{\pi} \leqslant x \end{cases} \tag{14}$$

In both cases, because of the invariance of x with length-scaling, only the amplitude of the Q-curve is affected by the nuclear charge. Eq. (13) is plotted in Fig. 1 for the Dirac and Becke functionals defined by (3) and (4), respectively, along with Eq. (14) for comparison.

The similarity of the plots is striking and indicates that each level of theory is attributing exchange energy to the same regions in the ion. The extremum of the Dirac Q-curve occurs at $x = 2\sqrt[3]{\pi}\ \mathrm{e}^{2/5} \approx 4.37$ and the rapid decay of all three of these curves shows why the asymptotic ($x \to \infty$) behaviour of a density functional usually

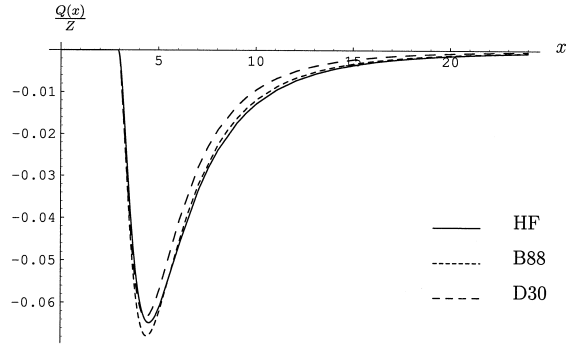

Fig. 1. Q-curves for the hydrogen-like ions for the HF, B88 and D30 functionals.

has a negligible effect on the energy of a system. No contribution is made from $x < 2\sqrt[3]{\pi}$ as these values of the reduced gradient do not occur in hydrogenic densities.

4. Numerical Q-curves

In general, the sets Ω_χ are disconnected regions that defy a closed form description, and as a result the generation of Q-curves for molecules is much more difficult than for spherical systems.

Although the use of numerical quadrature grids is normally a liability, it proves to be an asset in the present context. If we approximate Eq. (1) by the expression

$$E_X = \sum_i w_i \, \rho(\boldsymbol{r}_i)^{4/3} g(x(\boldsymbol{r}_i)) \tag{15}$$

where the w_i are integration weights, the gradient and an energy contribution may be calculated at each grid point and a representation of $q(x)$ in terms of delta functions constructed. The numerical noise associated with the integration grid may be smoothed by taking a moving average of the data.

Fig. 2 shows examples of these plots. In each case, the data were obtained by applying the Dirac exchange functional to UHF/6-311 + G(2df,p)//MP2/6-31G(d) densities and using the SG-1 grid [12]. An accurate analysis of the fine structure in the plots is difficult due to their numerical nature; however, some shell structure is apparent in larger atoms, and greater contributions to the energy arise from smaller x values for the

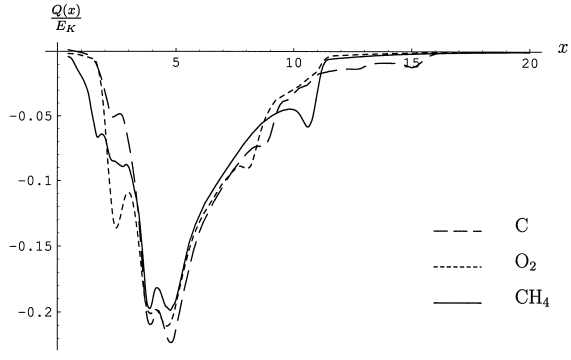

Fig. 2. $Q(x)/E_X$ for C, O_2 and CH_4 for the D30 functional

molecules. Their purpose here is to show that the general features of the Q-curves for many electron systems are similar to those for the single-electron hydrogenic ions. The characteristic peak around $x \approx 5$ is evident, as is the rapid decay beyond this value.

It is clear from these curves why the G96 functional [13] (which is non-analytic at the origin and has an unbounded potential in the Rydberg regions of the molecule) yields chemistry so close to the well behaved B88 [4] functional. The $g(x)$ functions for these functionals are almost identical over the energetically important region of $3 < x < 8$.

5. Ab initio functionals

How does one construct an ab initio density functional? The original approach taken by Dirac and others was to select a reference density and then find a functional which, in some limit, exactly reproduces a selected property. This is the path that we, too, will follow.

Which functional form should we choose? We have selected the form given by Eq. (1). It is simple, both conceptually and computationally, and, although it is known [8] that the true density functional for exchange is not of this form, it has proved itself useful in practice and is widely used.

Which property should we seek to reproduce? Given the simple functional form that we have chosen, it would be unwise to expect it to be capable of satisfying a demanding set of exact conditions. For example, Gill and Pople showed that, although it is mathematically possible for a functional of this form to yield both the exact exchange energy and the exact exchange potential of the hydrogen atom [8], the resulting functional is physically non-sensical. Instead, noting that the reduced gradient x is the key ingredient in Eq. (1) and that there is little variation in the Q-curves from molecule to molecule, we will stipulate that the functional should exactly reproduce the HF gradient spectrum of our reference density, i.e.

$$Q_{\mathrm{GG99}}(x) = Q_{\mathrm{HF}}(x) \tag{16}$$

Which reference density should we choose? The traditional choices, of course, have been the uniform electron gas (UEG) and the almost uniform electron gas and these have yielded the LSDA and its various gradient-corrected forms. It is well known, however, that these are poor models for the highly inhomogeneous electron densities that arise in atomic and molecular systems and it was this that led Gill and Pople [8] and Lee, Yang and Parr [14] to adopt the hydrogen and helium atoms, respectively, as their reference densities. For the same reason, we have chosen to abandon the UEG in the present work. Although the hydrogenic density might seem a natural choice, it is unsuitable for our present purposes because it does not contain any low-x regions. In fact, Eq. (12) shows that $x \geqslant 2\sqrt[3]{\pi}$ everywhere.

Since we seek a functional that performs well in chemical applications, it seems reasonable to choose a reference density that resembles the valence regions of an atom. It is well known [15] that the potential felt by a valence electron can be quite accurately modelled by an effective core potential (ECP) and this is widely exploited in quantum-chemical calculations involving heavy atoms [16]. It is therefore plausible that the electron density generated by an ECP might be a suitable reference density.

An ECP is a sum of a short-range part (normally a sum of gaussians) and a long-range part that tends exponentially to $-1/r$. We therefore sought a model potential $V(r)$ of this type that is sufficiently simple that the associated one-electron Schrödinger equation can be solved analytically. It turns out that the potential

$$V(r) = -\left(\mathrm{sech}(r)^2 + \tanh(r)/r\right) \tag{17}$$

is of the required form and yields the normalized ground-state wavefunction

$$\psi(r) = \sqrt{3/\pi^3}\ \mathrm{sech}(r) \tag{18}$$

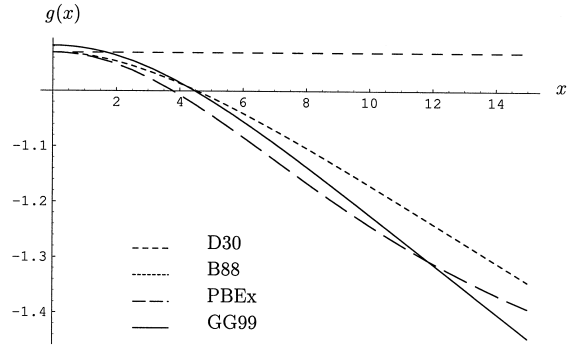

Fig. 3. The $g(x)$ functions for the D30, B88, PBEx and GG99 functionals ($0 < x < 15$).

with energy $E = -1/2$. On this basis, we decided to use

$$\rho(\mathbf{r}) = 3\,\mathrm{sech}^2(r)/\pi^3 \tag{19}$$

as our reference density. Notwithstanding its simplicity, we suspect that it is likely to be a better reference system than either the UEG or the hydrogen atom.

Having defined our reference system and method, it is prudent to reflect on the approximations made and on the deficiencies in our approach. We have assumed that exchange is a single-orbital phenomenon, and that this can be accurately modeled by an isolated valence electron. The multi-orbital component of the exchange energy will increase systematically with the number of electrons, and its neglect will result in errors that behave similarly. However, the valence electrons of larger systems lend themselves to a more accurate description by the density in Eq. (19). From this we expect that errors in the total energy will increase with system size but, because the bulk of the error is due to core electrons, these errors will largely cancel when considering energy differences [17].

The reduced gradient for the density (19) is given by

$$x(r) = 2\pi \sinh(r) \sqrt[3]{\mathrm{sech}(r)/3} \tag{20}$$

and the Ω_χ are spherical shells. Performing the integrations in Eqs. (7) and (10) and substituting into Eq. (16) we obtain an equation that can then be solved for $g_{\mathrm{GG99}}(x)$, which is most conveniently expressed in the form

$$g_{\mathrm{GG99}}(x) = -\frac{\pi^2 - 12\,r\log(1+\mathrm{e}^{-2r}) + 12\,\mathrm{L}_2(-\mathrm{e}^{-2r})}{2\sqrt[3]{3}\,\pi\,r\,\mathrm{sech}(r)^{2/3}} \tag{21}$$

where L_2 denotes the dilogarithm function and r is found by inverting (20), and given explicitly by

$$r = \mathrm{arcsinh}\left(\frac{\sqrt[4]{3}\,x\sqrt{x^2 + \left(4\sqrt{3}\,\pi^3 + \sqrt{48\pi^6 - x^6}\right)^{2/3}}}{2\sqrt{2}\,\pi^{3/2}\left(4\sqrt{3}\,\pi^3 + \sqrt{48\pi^6 - x^6}\right)^{1/6}}\right) \tag{22}$$

A plot of the new $g(x)$ in (21) is given in Fig. 3 and compared with corresponding plots for the Dirac and Becke functionals and the exchange component of the PBE functional (PBEx) [9].

The new $g(x)$ is similar to the Becke function; both are even functions, behave asymptotically as $O(x/\log(x))$ and cross at $x \approx 4.2$, which is in the most important region energetically. The Taylor series for the GG99 $g(x)$ begins

$$g_{\mathrm{GG99}}(x) = -0.9179 - 0.004492\,x^2 + 0.00002042\,x^4 + \ldots \tag{23}$$

whilst that for B88 begins

$$g_{\mathrm{B88}}(x) = -0.9305 - 0.004200\,x^2 + 0.0001058\,x^4 + \ldots \quad (24)$$

The curvature of these functions at the origin differs by only 0.0003, and our derivation incidentally provides some theoretical justification for the empirically chosen parameter, $b = 0.0042$, in the B88 functional.

We would not expect the GG99 functional to be correct for the UEG, so it is interesting to note that $g(0) \approx 0.92$ for the new functional, and that it therefore underestimates the exchange energy for the UEG by roughly 1%. The recently developed EDF1 [3] functional is also slightly imperfect for the UEG, but Adamson et al. established that this actually leads to superior chemistry.

6. Results and discussion

The GG99 functional has been implemented a modified version of the Q-Chem program [18], and has been used to calculate atomic exchange energies for the first 18 atoms (Table 1) and atomisation energies for the the molecules in the G2-1 set [19] plus H_2 (Table 2). All calculations were performed using MP2/6-31G(d) geometries, the 6-311 + G(3df,2p) basis and SG-1 [12] quadrature grid. The exchange energies in Table 1 were calculated by applying each functional to HF/6-311 + G(3df,2p) densities. All calculations for the atomisation energies were performed self-consistently [20] and use the HF zero-point vibrational energies from Ref. [19].

Table 1
Atomic exchange energies in mE_h

	HF[a]	ΔD30[b]	ΔB88[c]	ΔPBEx[d]	ΔGG99[e]
H	−313	45	3	7	−4
He	−1026	142	0	12	−24
Li	−1781	243	6	24	−34
Be	−2666	354	9	31	−48
B	−3768	473	9	37	−65
C	−5075	590	9	45	−76
N	−6604	706	10	54	−83
O	−8212	832	−6	45	−114
F	−10037	954	−20	40	−136
Ne	−12098	1073	−32	39	−149
Na	−14018	1234	−11	69	−136
Mg	−15992	1383	−6	80	−140
Al	−18091	1542	5	101	−137
Si	−20303	1696	12	120	−135
P	−22641	1849	20	139	−129
S	−25033	2011	25	156	−129
Cl	−27541	2166	26	170	−129
Ar	−30183	2321	31	188	−122
MAD[f]		1089.7	13.3	75.4	99.4

[a] UHF/6-311 + G(3df,2p) exchange energy.
D30–HF.
B88–HF.
PBEx–HF.
GG99–HF.
Mean absolute deviation.

Table 2
Atomisation energy differences, DFT-Expt. (in kcal/mol)

	Expt.	ΔS–VWN[a]	ΔB–LYP[b]	ΔPBE[c]	ΔGG–LYP[d]	ΔκGG–LYP[e]
O_2	118.0	−53.0	15.3	22.9	2.4	5.8
Cl_2	57.2	24.4	−0.3	7.0	−6.8	−3.7
SO	123.5	41.5	9.7	15.6	−0.3	4.2
S_2	100.7	33.1	5.6	13.0	−1.1	2.3
HOCl	156.3	46.4	4.5	11.2	−5.5	0.5
NH_2	170.0	26.3	8.0	7.3	5.7	9.6
$SiH_2(^1A_1)$	144.4	14.4	0.2	−3.8	−5.0	−2.0
$SiH_2(^3B_1)$	123.4	16.2	−0.4	1.0	−9.2	−5.4
H_2O	219.3	34.4	0.7	2.5	−2.3	4.1
NH_3	276.7	39.8	4.3	5.0	0.4	7.7
PH_2	144.7	21.0	4.8	1.8	−1.6	0.9
PH_3	227.4	28.0	0.7	−2.5	−8.0	−3.5
Si_2H_6	500.1	49.3	−10.2	−9.9	−35.8	−22.4
H_2CO	357.2	60.8	5.0	13.5	−10.3	0.9
SH_2	173.2	24.0	−1.7	−0.2	−5.4	−1.6
H_2O_2	252.3	66.2	7.5	13.9	−5.2	3.3
HF	135.2	21.5	0.5	1.6	−1.2	3.0
BeH	46.9	10.8	7.4	6.1	3.9	6.8
H_2NNH_2	405.4	77.8	9.6	15.8	−4.8	7.7
$CH_2(^1A_1)$	170.6	18.2	−0.6	−1.5	−4.0	0.2
$CH_2(^3B_1)$	179.6	22.8	0.0	4.9	−5.2	1.2
CH_3OH	480.8	75.1	−0.4	9.5	−19.3	−3.4
NH	79.0	11.9	6.0	5.1	5.2	6.7
SiH_3	214.0	19.7	−2.7	−4.4	−13.5	−8.2
SiH_4	302.8	25.4	−4.1	−8.1	−17.3	−10.0
F_2	36.9	38.2	9.7	13.4	0.0	2.1
HCN	301.8	48.6	8.4	14.5	−1.6	5.5
HCO	270.3	55.2	9.6	17.9	−4.0	4.3
LiF	137.6	17.5	1.5	0.3	−0.7	6.1
HCCH	388.9	54.6	−0.2	9.9	−11.5	0.4
H_2CCH_2	531.9	70.0	−1.7	9.7	−18.5	−1.9
H_3CCH_3	666.3	83.0	−6.7	6.6	−30.1	−9.1
NO	150.1	46.4	13.8	19.5	2.3	6.0
LiH	56.0	2.7	0.1	−4.4	1.6	2.9
N_2	225.1	36.9	10.5	13.7	1.7	3.8
Na_2	16.6	3.8	1.2	1.3	3.3	3.1
P_2	116.1	26.2	4.9	4.0	−1.4	−0.6
CO_2	381.9	85.6	12.7	29.3	−10.3	2.6
Li_2	24.0	−0.6	−3.6	−4.1	−0.4	−0.4
SiO	190.5	30.6	2.6	3.4	−4.6	0.8
CH	79.9	8.6	1.8	1.0	0.4	2.1
CH_3Cl	371.0	53.8	−3.7	7.1	−18.7	−6.5
Si_2	74.0	18.4	1.4	6.2	−5.5	−3.8
CN	176.6	39.4	10.3	16.6	0.7	6.0
CO	256.2	39.9	3.2	10.3	−7.9	−1.9
SO_2	254.0	74.7	7.1	20.5	−13.8	−4.0
ClF	60.3	33.1	5.6	10.6	−3.3	0.2
SC	169.5	30.9	0.9	8.3	−6.6	−2.6
OH	101.3	17.8	3.4	3.7	1.9	4.6
HCl	102.2	14.4	−1.5	0.6	−2.7	−0.2
CH_3SH	445.1	63.6	−5.1	5.9	−22.1	−8.4
NaCl	97.5	6.5	−5.7	−3.0	−8.5	−4.3
CH_3	289.2	32.7	0.4	3.9	−6.2	2.3

Table 2 (continued)

	Expt.	ΔS–VWN[a]	ΔB–LYP[b]	ΔPBE[c]	ΔGG–LYP[d]	ΔκGG–LYP[e]
ClO	63.3	39.4	10.6	16.8	0.4	3.4
CH_4	392.5	43.1	−2.4	1.3	−12.2	−1.1
H_2	103.3	3.8	0.2	−4.4	2.7	3.8
MAD[f]		35.39	4.66	8.21	6.88	4.10
MD[g]		35.37	2.83	6.56	−5.71	0.35

[a] S–VWN–Expt.
[b] B–LYP–Expt.
[c] PBE–Expt.
[d] GG–LYP–Expt.
[e] κGG–LYP–Expt., $\kappa = -0.047$.
[f] Mean absolute deviation.
[g] Mean deviation.

For some linear open-shell systems, convergence problems were encountered when electrons oscillated between degenerate orbitals. These were overcome by using a converged guess density, and then fixing the electronic orientation throughout the self-consistent field calculation [21].

Both D30 and PBEx systematically underestimate the magnitude of the exchange energy and B88 also shows this tendency. GG99 contrasts this with a systematic overestimation of the exchange energy. Without exception, the pattern in the energies is GG99 < HF < PBEx < D30. For GG99 the first-row atoms show a monotonic increase in absolute error with increasing atomic number, while the error in the second-row atoms is almost constant.

When paired with the Lee–Yang–Parr (LYP) correlation functional, GG99 affords atomisation energies that on average are superior to both LSDA and PBE [22], [1] but inferior B-LYP. Fig. 3 shows the $g_{\mathrm{GG99}}(x)$ function lies above $g_{\mathrm{D30}}(x)$ in the region $0 < x < 1.7$. This results in an underestimation of the (negative) exchange energy in the bonding regions of the molecule, and explains the underbinding tendency of GG–LYP. This is exacerbated in larger molecules where a greater proportion of the density lies in bonding regions.

The underbinding of the present model can be alleviated by including some of the multi-orbital exchange neglected in GG99. The Dirac exchange functional is based on the UEG and is well suited to modeling this exchange. We have therefore explored the usefulness of empirically augmenting GG99 with a fraction of D30.

Mixing in Dirac exchange is equivalent to shifting the $g_{\mathrm{GG99}}(x)$ curve vertically, which adds exchange contributions uniformly to all values of the reduced gradient. This effect largely cancels between atoms and molecules, except in the flat bonding regions, and consequently leads to greater binding. The amount of mixing is determined by a single parameter, κ, and the shifted functional, κGG99, is given by the following modification of GG99,

$$E[\,\rho\,]_{\kappa GG99} = \int \rho(\boldsymbol{r})^{4/3}\left(\kappa + g_{\mathrm{GG99}}(x)\right)\,\mathrm{d}\boldsymbol{r} \tag{25}$$

A simple minimisation gives $\kappa = -0.047$, and the atomisation energies for the resulting shifted functional are given in the final column of Table 2. The effect of mixing in Dirac exchange is significant; the mean absolute deviation drops by 40%. The shifted GG99 functional is no longer ab initio; however, its single

[1] Our implementation of the PBE functional difers from that published in that it uses the VWN functional (fifth parameterisation) for the UEG correlation component.

parameter enters in the simplest possible way, and appears to compensate for one, or both, of the deficiencies in the model.

7. Conclusions

This Letter has discussed the notion of Q-curves and considered two uses of the information they contain. Firstly, they illustrate clearly which values of the reduced density gradient are energetically important, and in particular high values (corresponding to the Rydberg regions of the molecule) contribute little energy. Relying on asymptotic limits to determine the form of an approximate functional may therefore place unnecessary constraints on the functional, if it is of the same form as Eq. (1).

Secondly, with this in mind, Q-curves provide a natural mechanism for deriving ab initio gradient corrected functionals, which does not oblige the functional to make up for the inadequacies in its form. We have used this approach in conjunction with a simple single-electron model density to derive the GG99 functional, which yields the exact exchange energy when applied to this density. The major deficiency in this approach is the neglect of multi-orbital contributions to the exchange energy. Inclusion of a small fraction of Dirac exchange provides a straightforward way to remedy this.

We have focused on the simple density given by (19) because it represents the density of a valence s-electron. However, Q-curves provide a simple mapping from *any* spherical monotonic one-electron density to an exchange functional of the form (1), and we note that the 'optimal' choice of model density remains an open question.

Acknowledgements

One of us (A.T.B.G.) gratefully acknowledges financial support from Q-Chem, Inc., the Cambridge Commonwealth Trust and the ORS Awards Scheme. This research has been partially supported by an SBIR grant to Q-Chem, Inc. from the National Science Foundation. ATBG would also like to acknowledge M. Ernzerhof for helpful discussions concerning the PBE functional.

References

[1] H.L. Schmider, A.D. Becke, J. Chem. Phys. 108 (1998) 9624.
[2] D.J. Tozer, N.C. Handy, J. Chem. Phys. 108 (1998) 2545.
[3] R.D. Adamson, P.M.W. Gill, J.A. Pople, Chem. Phys. Lett. 284 (1998) 6.
[4] A.D. Becke, Phys. Rev. A 38 (1988) 3098.
[5] M. Levy, A. Gorling, Phys. Rev. A 53 (1996) 3140.
[6] P.A.M. Dirac, Proc. Cambridge Phil. Soc. 29 (1930) 376.
[7] S.H. Vosko, L. Wilk, M. Nusair, Can. J. Phys. 58 (1980) 1200.
[8] P.M.W. Gill, J.A. Pople, Phys. Rev. A (1993) 2383.
[9] J.P. Perdew, K. Burke, M. Ernzerhof, Phys. Rev. B 77 (1996) 3865.
[10] A. Zupan, J.P. Perdew, K. Burke, M. Causà, Int. J. Quantum Chem. 61 (1997) 835.
[11] A. Zupan, K. Burke, M. Ernzerhof, J.P. Perdew, J. Chem. Phys. 106 (1997) 10184.
[12] P.M.W. Gill, B.G. Johnson, J.A. Pople, Chem. Phys. Lett. 209 (1993) 506.
[13] P.M.W. Gill, Mol. Phys. 89 (1996) 433.
[14] C. Lee, W. Yang, R.G. Parr, Phys. Rev. B 37 (1988) 785.
[15] L.R. Kahn, P. Baybutt, D.G. Truhlar, J. Chem. Phys. 65 (1976) 3826.
[16] M. Krauss, W.J. Stevens, Ann. Rev. Phys. Chem. 35 (1984) 357.
[17] J.A. Pople, R.D. Adamson, P.M.W. Gill, J. Phys. Chem. 100 (1996) 6348.

[18] C.A. White, J. Kong, D.R. Maurice, T.R. Adams, J. Baker, M. Challacombe, E. Schwegler, J.P. Dombroski, C. Ochsenfeld, M. Oumi, T.R. Furlani, J. Florian, R.D. Adamson, N. Nair, A.M. Lee, N. Ishikawa, R.L. Graham, A. Warshel, B.G. Johnson, P.M.W. Gill, M. Head-Gordon, Q-Chem, version 1.2, Q-Chem, Inc., Pittsburgh, PA, 1998.
[19] L.A. Curtiss, K. Raghavachari, G.W. Tracks, J.A. Pople, J. Chem. Phys. 94 (1991) 7221.
[20] J.A. Pople, P.M.W. Gill, B.G. Johnson, Chem. Phys. Lett. 199 (1992) 557.
[21] A.T.B. Gilbert, G.B.W. Gill, P.M.W. Gill, in preparation.
[22] M. Ernzerhof, G.E. Scuseria, J. Chem. Phys. 110 (1999) 5029.